



MRI in Spine Infection

5

M. K. Jesse and Corey K. Ho

Introduction

Spine infection is a rare and often misdiagnosed condition with critical implications for patient care. Over the last 30 years, spine infection has steadily increased not only due to the rising epidemic of intravenous drug use and immune disorders but also from the inevitable side effects of advancements in modern medicine. Patients with debilitating chronic disease and severe immune compromise are experiencing longer life expectancy leading to a greater number of patients at high risk for infection. Surgical and procedural instrumentation procedures in the spine are steadily increasing, offering life-altering benefits to many patients but also elevating the number of high-risk patients [1]. Prompt identification and characterization of spine infection is essential to optimize patient outcomes. Navigation of infectious and non-infectious diseases in the spine poses not only a clinical dilemma because of the substantial overlap in the clinical symptomatology and laboratory findings but also poses a substantial diagnostic dilemma because of the confusing overlap in the imaging features. It is critical for all providers to understand the nuances and subtleties in imaging features of infectious disease processes to ensure accurate diagnosis

and treatment, especially in this high-risk patient population.

Pyogenic Spondylodiscitis (Bacterial Spondylodiscitis)

Pathophysiology

Pyogenic spondylodiscitis is defined as the infection of a vertebral body and intervertebral disc with or without involvement of the adjacent epidural space and paraspinal soft tissues. It is unfortunately common, affecting 2 per 100,000 each year with a propensity to affect intravenous drug users, diabetics, immune-compromised patients, and patients with recent surgery or intervention [2, 3]. Men are two to three times more often affected for reasons that are not entirely understood [4]. Early diagnosis of pyogenic spondylodiscitis is critical as the mortality reaches 17% according to some studies and even higher when associated with advanced comorbidities [4–6].

Staphylococcus aureus is overwhelmingly the most common causative agent, seen in 40–70% of cases and typically transmitted to the spine via the bloodstream (hematogenous spread) [7, 8]. Hematogenous spread of infection occurs when organisms from the blood are deposited in the small arterioles of the endplates in adults and in the disc itself in very young children [9]. The deposition of bacteria at the endplates of adults

M. K. Jesse (✉) · C. K. Ho
University of Colorado Anschutz Campus,
Aurora, CO, USA
e-mail: mary.jesse@ucdenver.edu;
Corey.k.ho@ucdenver.edu

rapidly progresses to intradiscal infection due to the virulent proteolytic enzymes produced by common organisms like *S. aureus*.

Batson described an alternative mode of pathogen transit to the spine that occurs by way of retrograde venous flow from the genitourinary and gastroenteric tract introducing the less common *Enterococcus* and *Escherichia* genus to the spine. *Pseudomonas* and *Streptococcus* species have been shown to seed to the spine in patients with a history of intravenous drug use and diabetes, respectively.

Acquiring blood cultures in suspected cases of spondylodiscitis is critically important as culture positivity is present in 50–70% of spondylodiscitis cases. The organism isolated from the blood is identical to that isolated from bone/disc biopsy 70–80% of the time [4]. Positive blood cultures arguably can negate the need for bone biopsy in straightforward cases.

Imaging in Pyogenic Spondylodiscitis

Various imaging modalities including radiographs, computed tomography (CT), magnetic resonance imaging (MRI), and nuclear medicine bone scan may be utilized in the evaluation of spine infection. Each of these imaging modalities offers unique benefits and limitations that should be considered prior to utilization. Many modalities may be used in tandem to increase specificity and sensitivity.

Radiographs

Radiographs of the spine in the setting of spondylodiscitis are a reasonable first step in assessment. Providing fast and inexpensive evaluation is an attractive benefit of radiographs. However, radiographs may be prohibitively insensitive in the first 2 weeks after inoculation [10]. A normal radiograph in a patient with suspected osteomyelitis should not be considered an indication of disease absence. The temporal evolution of radiographic changes in spondylodiscitis begins at about 7 days after infection onset where one may note only a

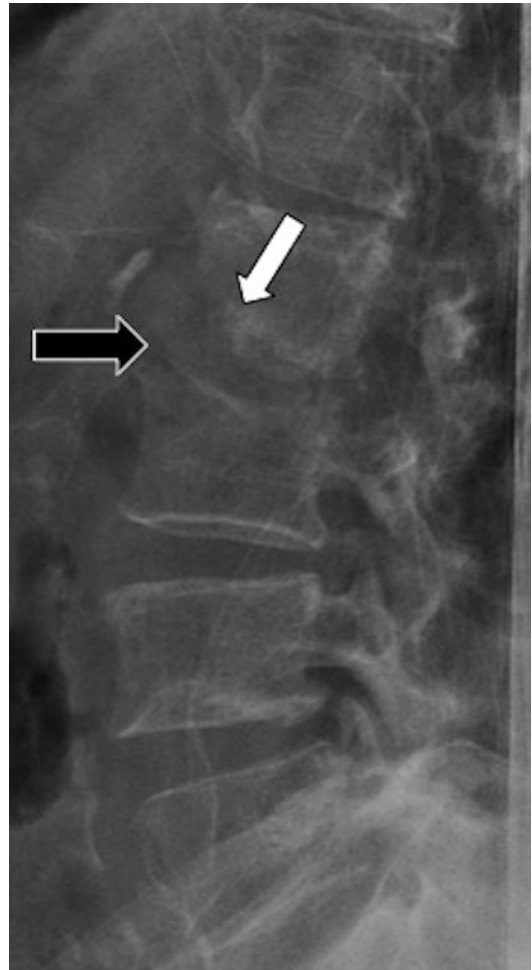


Fig. 5.1 Lateral radiograph of the lumbar spine demonstrates early disc height loss at L2–L3 (black arrow) in combination with ill-defined endplate erosions (white arrow), findings in keeping with discitis

subtle loss of intervertebral disc height. Over the next 1–2 weeks, this disc height loss will evolve to the more specific and sensitive finding of endplate irregularity and erosion typically occurring along the anterior margin [11] (Fig. 5.1).

Computed Tomography

Computed tomography (CT) can be useful as an adjunct to radiographs. The imaging features are similar and include focal osteopenia, disc height loss, cortical irregularity, and endplate erosions.

However, CT may illustrate these subtle findings earlier in the disease process due to the increased detail provided.

Keep in mind that sub-endplate cysts in the setting of degenerative disease may mimic the endplate erosions of infection. In spite of this, these findings can be differentiated through an understanding of the pathophysiology. Sub-endplate degenerative cysts, like virtually all degenerative disease processes in the skeleton, will demonstrate a well-defined sclerotic rim of bone production indicating a chronic process. By contrast, sub-endplate erosions in infection occur rapidly and aggressively with a preponderance of osteoclastic activity. Because of this, the margin of the erosion will be ill-defined and non-sclerotic, indicative of an acute process (Fig. 5.2).

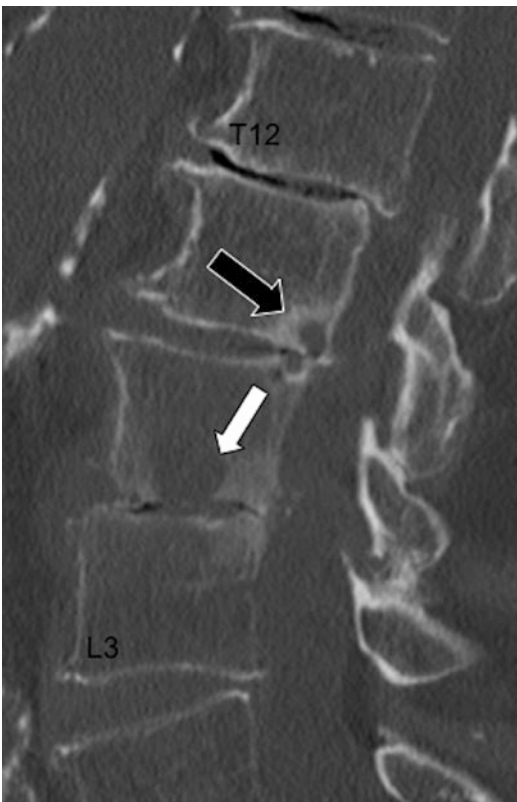


Fig. 5.2 Sagittal CT image of the lumbar spine demonstrates disc height loss at L2–L3 with focal acute erosion at the L2 endplate (white arrow). A non-infectious degenerative sub-endplate cyst at the posterior L1 vertebra can be differentiated from the infectious erosion by the clearly defined sclerotic rim (black arrow)

Paraspinal phlegmon and soft tissue inflammation is reflected on CT as fat stranding adjacent to the spine with loss of the intramuscular and perimuscular fat planes. The addition of contrast aids in detection of phlegmonous enhancement and epidural/paraspinal abscess formation. CT is limited in the evaluation of the postoperative patient with indwelling spinal fusion due to the potential for beam-hardening artifact and image degradation.

Nuclear Medicine

Nuclear medicine technetium-99-labeled methylene diphosphonate (^{99m}Tc -MDP) bone scan, or more generally termed bone scintigraphy, may be used to identify spondylodiscitis with increased sensitivity over CT and radiograph in the early phases of disease. Through the adsorption of radiotracer at the surface of hydroxyapatite crystals of bone matrix, bone scintigraphy identifies areas of high osteoblastic activity and bone remodeling with a high level of sensitivity (Fig. 5.3). ^{99m}Tc -MDP bone scan can detect areas of osteomyelitis as early as 48 h after the onset of infection with a sensitivity of 70–100% [12]. In addition, ^{99m}Tc -MDP bone scan may also help overcome the limitations of spine hardware in a postoperative patient. Bone scan, as opposed to CT and MRI, is not susceptible to metal artifact and therefore may be a reasonable choice for the evaluation of spondylodiscitis in a postoperative patient. The limitation of bone scintigraphy lies in the poor specificity and high false-positive rates. Any disease process resulting in a relative increase in osteoblast activity and hyperemia will result in a focal radiotracer uptake making it difficult to differentiate between infection and other degenerative, traumatic, or malignant disease processes.

$^{67}\text{Gallium}$ SPECT imaging may be added to routine bone scintigraphy in an attempt to increase the specificity of the exam in the setting of infection. Used primarily in the spine, $^{67}\text{Gallium}$ citrate isolates potential infection by binding to neutrophil membranes and siderophore chelates produced by bacterium. The routine use

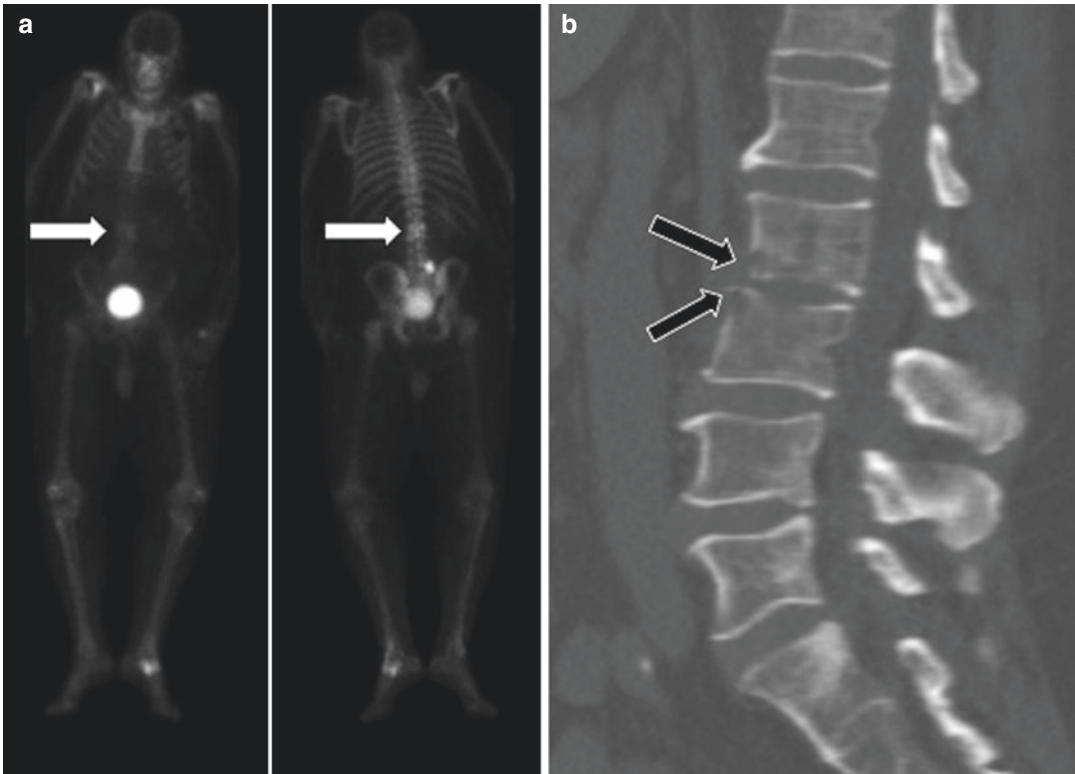


Fig. 5.3 A 46-year-old male with L2–L3 pyogenic spondylodiscitis. ^{99m}Tc -MDP whole-body bone scan (**a**) demonstrates increased radiotracer activity within the L2 and L3 vertebra (white arrows) in keeping with spondylodiscitis.

Sagittal CT image (**b**) demonstrates acute endplate erosions and relative osteopenia (black arrows), confirming the diagnosis of L2–L3 infectious spondylodiscitis.

of ^{67}Ga SPECT is limited, however, due to the high effective dose, long half-life, and poor spatial resolution of the scan [13]. It should also be considered that the target organ for ^{67}Ga citrate is the large bowel, which can obscure areas of interest depending on the location of the bowel.

^{18}F -FDG PET has an extremely high sensitivity for detecting spondylodiscitis and can arguably exclude the diagnosis of spondylodiscitis with a negative scan. Current literature has suggested a superiority of PET/CT over MRI both in specificity and sensitivity [14]. As the availability of this modality becomes more widespread, we may see PET replacing MRI as the modality of choice especially in patients with indwelling hardware and other MRI limitations.

Magnetic Resonance Imaging

Magnetic resonance imaging (MRI) is the current modality of choice for the evaluation of spondylodiscitis due to its high sensitivity (96%), high specificity (94%), and ability to provide detailed assessment of the paraspinal soft tissues and epidural space [15, 16]. Standard MR imaging protocols should include fluid-sensitive sequences such as T2-weighted spin echo or short tau inversion recovery (STIR) in axial and sagittal planes for the detection of fluid and edema. Fat saturation is often used in fluid-sensitive sequences to increase the sensitivity for detecting edema against a background of marrow and soft tissue fat [15]. The addition of T1-weighted fat-sensitive sequences in sagittal and/or axial planes is important to eval-

uate anatomic structures and detect replacement of marrow and soft tissue fat in the vertebra and neural foramen. Although these sequences may be sufficient for the diagnosis of spondylodiscitis, whenever possible, post-gadolinium contrast images should be included to improve detection of small epidural and paraspinal abscesses. A sample MRI protocol is illustrated in Table 5.1.

Pyogenic infection in the vertebral body results in an exudative proliferation within the bone that imbibes and replaces the normal intraosseous fatty marrow. This intraosseous exudate appears as increased fluid (T2 signal) in two consecutive vertebrae with concomitant confluent hypointense T1 signal in the marrow space (Fig. 5.3). Hyperintense T2 signal and confluent hypointense T1 signal are the quintessential imaging features of osteomyelitis anywhere in the skeleton but must be used with caution in the spine due to

the propensity to misdiagnose infection in otherwise benign conditions. Degenerative disc disease, for example, may also result in similar endplate signal characteristics known as Modic change [17, 18]. Evaluating the transverse and craniocaudal extent of the signal abnormality within the vertebra may help to increase diagnostic specificity. In a study by Malgorzata, corresponding signal abnormality on T1- and T2-weighted sequences involved 50% or more of the vertebral body in 89% of spondylodiscitis cases studied. In degenerative disease, the hyperintense T2 and hypointense T1 signal abnormalities are rarely seen involving more than half of the vertebra and more typically affect the bone immediately adjacent to the affected endplate (Fig. 5.4).

Gadolinium enhancement of the vertebra may be seen on post-contrast imaging and is expected to match the pattern of T2 signal. Contrast

Table 5.1 Sample magnetic resonance imaging (MRI) protocol for spine infection

Fluid-sensitive sequences	Fat-sensitive sequence	Post-contrast sequences
Sagittal T2-weighted with/without fat saturation	Sagittal T1-weighted without fat saturation	Sagittal T1-weighted with fat saturation
STIR with fat saturation		Axial T1-weighted with fat saturation
Axial T2-weighted without fat saturation		

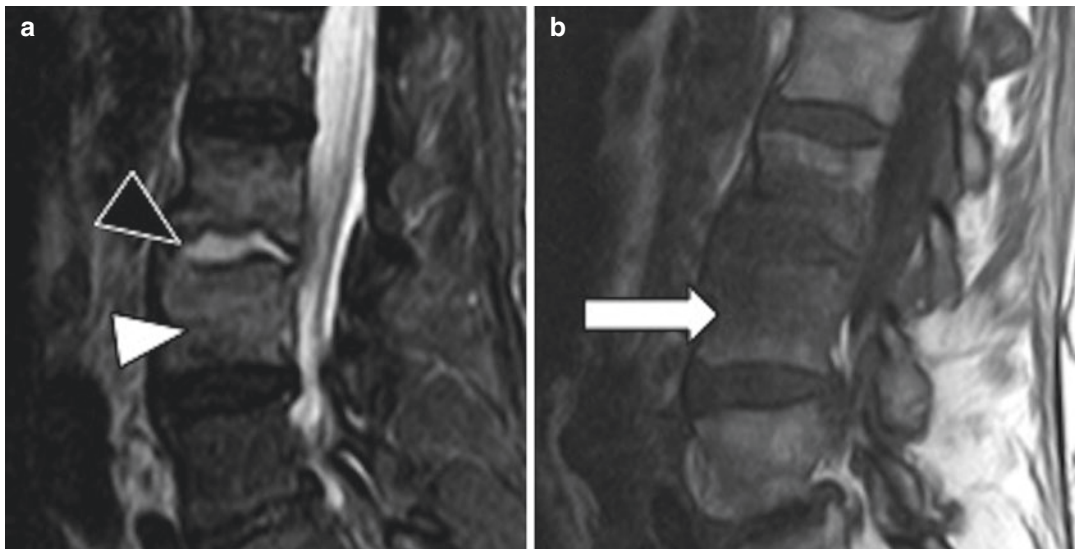


Fig. 5.4 A 56-year-old male with L2–L3 pyogenic spondylodiscitis. Sagittal STIR fat-saturated MR image (**a**) demonstrates diffuse hyperintense signal >50% of the vertebral body height (white arrowhead) and uniform

increased signal within the affected intervertebral disc (black arrowhead). Sagittal non-fat-saturated T1 image (**b**) demonstrates confluent hypointense T1 signal occupying >50% of the vertebral height (white arrow)

enhancement of the edematous vertebra alone does not assist in narrowing the differential diagnosis, as essentially all bone marrow edema will enhance similarly regardless of the origin of the edema. Post-contrast images do however assist in the identification of paraspinal inflammation as well as psoas and epidural abscess, the most specific findings in the diagnosis of spondylodiscitis [19]. Abscesses, whether outside or within the canal, demonstrate internal hyperintense T2 signal with peripheral contrast enhancement (Fig. 5.5).

Signal intensity within the intervertebral disc is like that of the bone. T2-weighted images demonstrate hyperintense T2 intradiscal signal intensity usually accompanied by uniform hypointense T1 signal and enhancement on post-contrast images. Disc enhancement patterns include homogeneous disc enhancement, patchy heterogeneous areas of disc enhancement, or non-enhancement in advanced disease [20].

Some authors have described effacement of the central fibrous band of the intervertebral nucleus pulposus, the intranuclear cleft, as a sign of disc infection although this finding is often absent in early stages of disease [21] (Fig. 5.6).

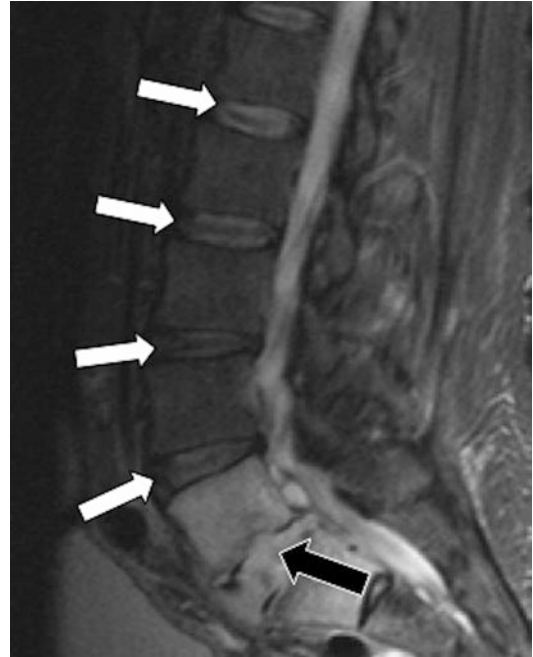


Fig. 5.6 A 44-year-old male with pyogenic spondylodiscitis involving L5–S1. Sagittal STIR fat-saturated MR image demonstrates normal fibrous intranuclear clefts (white arrows) within the uninvolved intervertebral discs. The intranuclear cleft at L5–S1 is effaced (black arrow)

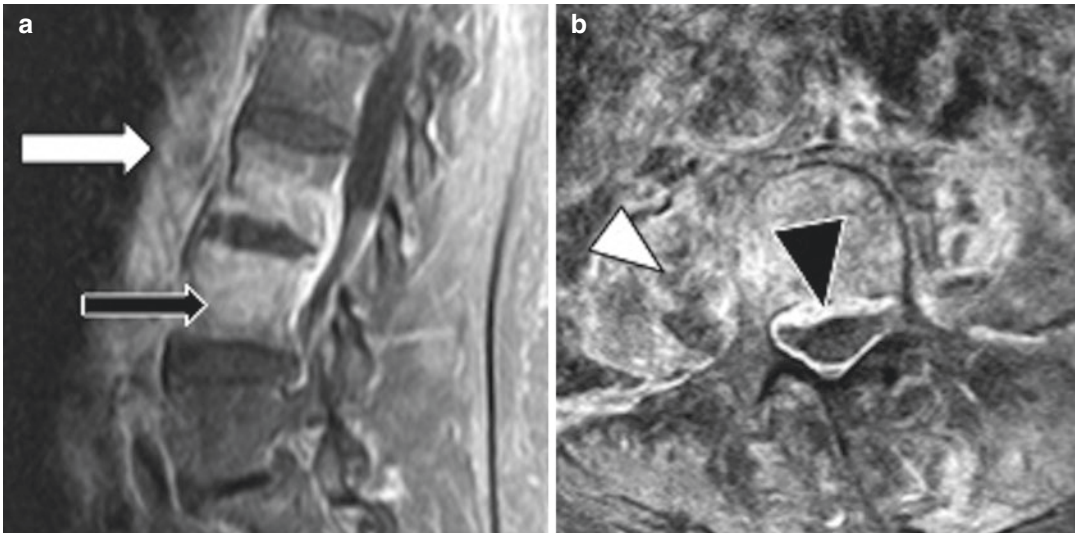


Fig. 5.5 A 56-year-old male with L2–L3 pyogenic spondylodiscitis. Sagittal T1 fat-saturated post-contrast image (a) demonstrates diffuse vertebral body enhancement (black arrow) and paraspinal soft tissue edema/phlegmon

(white arrow). Axial T1 fat-saturated post-contrast image (b) demonstrates a peripherally enhancing right paraspinal abscess (white arrowhead) and epidural thickening with enhancement (black arrowhead)

Temporal Changes of Pyogenic Spondylodiscitis

When classic imaging features of pyogenic spondylodiscitis are present, there is usually very little diagnostic uncertainty. However, diagnostic problems arise during early- and late-stage disease, where imaging features may be subtle or confusing with overlapping findings. Understanding the expected temporal changes of spondylodiscitis is critical in determining the appropriate diagnosis and treatment plan.

Not surprisingly, spondylodiscitis can be quite subtle in the early stages and may mimic other conditions like degenerative disc disease, acute Schmorl's nodes, malignancy, or trauma. In hematogenous spread of pyogenic spondylodiscitis, the earliest MRI findings of inoculation include hazy hyperintense T2 signal at the anterior or posterior endplates in a single vertebra or at two consecutive vertebral body endplates [21, 22]. This signal abnormality reflects the initial end arteriole bacterial deposition prior to the enzymatic endplate breakdown. Other subtle findings include faint paraspinal soft tissue edema and focal epidural enhancement. These early findings are uniformly non-specific, and infection can only be suggested and not confirmed with a single MRI evaluation. In individuals with high risk history or concerning clinical picture, a repeat MRI in 8 days is recommended to exclude infection in the setting of subtle MRI changes. Any interval progression in the imaging features over this 8-day period should be considered highly suspicious for an infectious etiology [23].

The other period of diagnostic uncertainty lies in the later stages of disease after the initiation of antibiotic therapy. Misunderstandings as to the expected temporal evolution of MRI findings in the post-treatment phase are dangerous and may result in unnecessary surgery [24]. Recent evidence suggests that many MR imaging features of spondylodiscitis worsen in the post-treatment period despite the initiation of appropriate antibiotic therapy and clinical improvement [25–27]. Bone marrow edema, enhancement of the vertebral body and disc, endplate erosions, and loss of intervertebral disc height may be expected to

worsen for up to 4–6 months following appropriate and effective antibiotic therapy. The most reliable feature of appropriate therapy is the improvement or resolution of soft tissue and/or epidural abscess which tends to occur in the earlier stages of therapy. Worsening of an abscess following treatment would therefore be the most reliable indicator of treatment failure [25, 26] (Fig. 5.7)

Tuberculous Spondylodiscitis

Pathophysiology

Tuberculous (mycobacterial) spondylodiscitis (TS) is a rare but serious condition that is unfortunately common in underdeveloped countries but has been steadily rising in incidence in all countries around the world [28]. Tuberculosis of the spine accounts for only 1% of cases of tuberculosis but makes up 25–60% of the skeletal involvement of the disease [29]. The clinical presentation of TS is more insidious and mild, often without back pain and fever or the profound elevations in inflammatory markers or leukocytosis seen with pyogenic spondylodiscitis. Because of this insidious course, patients suffering from TS may not present until in very late stages of disease, sometimes 12 months or more after initial inoculation, often after substantial destruction has occurred [30, 31].

Differentiating TS from pyogenic spondylodiscitis is of critical importance as to not delay appropriate therapy but can be difficult as there is overlap in the imaging features. Unlike pyogenic spondylodiscitis, TS is most often transmitted to the spine via Batson's venous plexus rather than through the end arterioles. Venous transmission of bacteria results in primary inoculation at the anterior-inferior endplates of the cancellous vertebral body. It is suggested that tuberculous spondylodiscitis may also differ from pyogenic spondylodiscitis in that it favors the thoracic spine. The largest cohort demonstrates a thoracic predominance with 56% of cases presenting from T1–T12 and only around 20% presenting in the lumbar spine [32, 33]. This thoracic predilection,

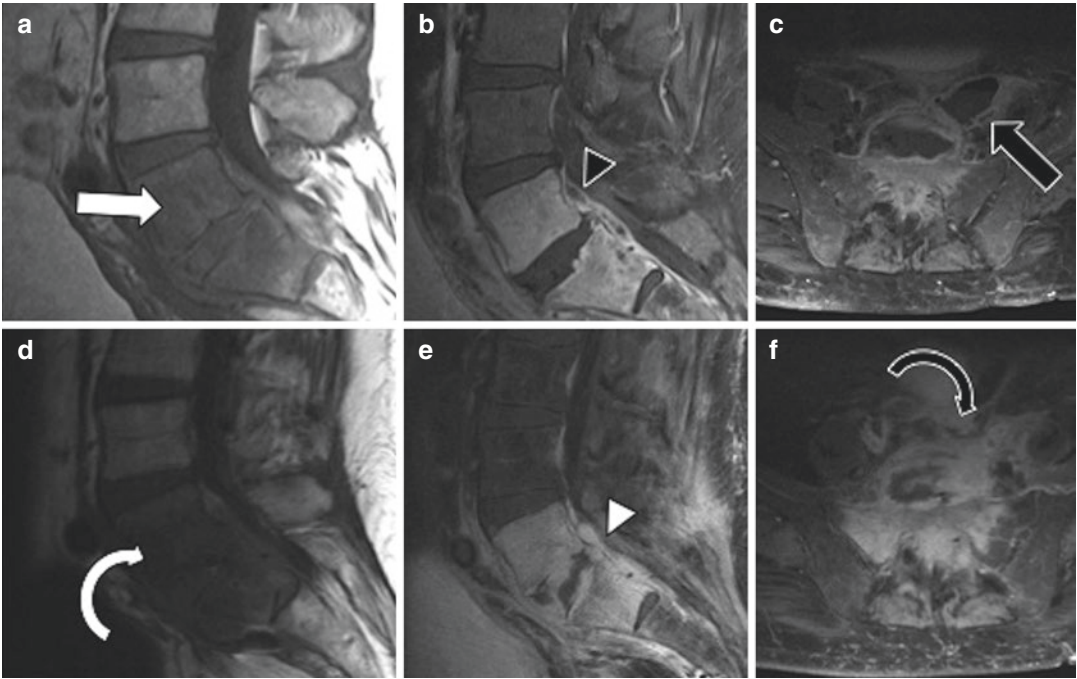


Fig. 5.7 A 54-year-old male with *S. aureus* spondylodiscitis of L5–S1. Pre-treatment sagittal T1 (a), sagittal T1 fat-saturated post-contrast (b), and axial T1 fat-saturated post-contrast (c) images of the spine demonstrate confluent hypointense T1 signal (white arrow) and vertebral body enhancement with small epidural abscess (black arrowhead) and large paraspinous abscess (black arrow). Repeat sagittal T1 (d), sagittal T1 fat-saturated post-

contrast (e), and axial T1 fat-saturated post-contrast (f) images at 5 weeks following appropriate antibiotic therapy and clinical improvement demonstrate worsening hypointense T1 signal (white arrowhead) and worsening enhancement and endplate destruction (white curved arrow). There is complete resolution of the small epidural abscess (white arrowhead) and paraspinous abscess (black curved arrow)

however, has been debated with several reports demonstrating equal involvement of the thoracic and lumbar spine in mycobacterial cases [34].

Imaging in Tuberculous Spondylodiscitis

One of the key imaging features differentiating tuberculous spondylodiscitis from pyogenic spondylodiscitis is a product of the inability of mycobacterium to produce the proteolytic enzymes which are common in pyogenic forms of the disease. The absence of proteolytic enzymes prevents the mycobacterial species from traversing dense fibrous structures around the spine such as the fibrous annulus of the intervertebral disc and the paraspinous ligaments [35]. Rather than entering and destroying the disc,

mycobacterium spreads in the spine via a subligamentous course typically under the anterior longitudinal ligament to the adjacent vertebral level, sparing the intervertebral discs until very late stages of disease. The absence of disc destruction and the sub-ligamentous transmission allows for multiple consecutive levels (three or more) of the spine to be involved simultaneously [32, 33]. This is contrary to pyogenic disease which typically involves no more than two consecutive spinal levels with significant disc destruction early in the disease process.

Radiographs

Radiographs serve as an acceptable initial screening tool in the evaluation of tuberculous spondylodiscitis but can be insensitive in early disease.



Fig. 5.8 A 37-year-old female with *Mycobacterium tuberculosis* infection of the spine. Lateral radiograph demonstrates multilevel vertebral body collapse (white arrow) with severe gibbus kyphotic deformity. Subtle findings of relative vertebral body osteopenia can be appreciated at the adjacent levels (black arrow)

The earliest findings of TS include relative osteopenia of the vertebra, an extremely difficult finding to appreciate when disease is localizing to the upper or mid thoracic spine due to the overlapping soft tissue and bone. In later stages of disease, more classic radiographic features of multilevel vertebral body involvement and gibbus deformity can be appreciated. Gibbus deformity is a term reserved for advanced cases of TS and is used to describe the severe kyphotic angulation produced by multilevel vertebral body collapse (Fig. 5.8).

Magnetic Resonance Imaging

MRI in tuberculous spondylodiscitis is a valuable tool in diagnosis. Imaging features differentiating this disease process from pyogenic spondylodiscitis are largely related to the unique subligamentous spread of infection discussed above. Often on MRI, hyperintense T2 signal can be



Fig. 5.9 A 37-year-old female with tuberculous spondylodiscitis. Sagittal STIR fat-saturated image demonstrates hyperintense T2 signal within the mid-thoracic vertebral body. Hyperintense T2 signal can be seen undermining the anterior longitudinal ligament in keeping with subligamentous spread (white arrow)

seen tracking beneath the anterior longitudinal ligament to the adjacent vertebral body, sparing the intervertebral discs and confirming this unique behavior (Fig. 5.9). Inoculation of multiple consecutive levels (three or more) is also suggestive of a mycobacterial organism over pyogenic disease. Imaging features within the vertebra are similar to that of pyogenic spondylodiscitis with hyperintense T2 signal, enhancement, and confluent hypointense T1 signal occupying the majority of the vertebral marrow space [32, 33].

Intervertebral abscess appearing as a variable size hyperintense T2 marrow lesion with peripheral enhancement is a feature suggestive of TS and should be considered suspicious for atypical infection [32, 33] (Fig. 5.10) The MRI appearance of paraspinal abscesses may also help to differentiate these two disease processes. Specifically, the post-contrast pattern of rim enhancement has been shown to correlate with the underlying etiology. Paraspinal abscesses in tuberculous infection demonstrate a thin peripheral rim enhancement that is homogeneous across the entire abscess wall. This in distinction to pyogenic abscesses which typically demonstrate a thick and irregular enhancement along the wall [32].

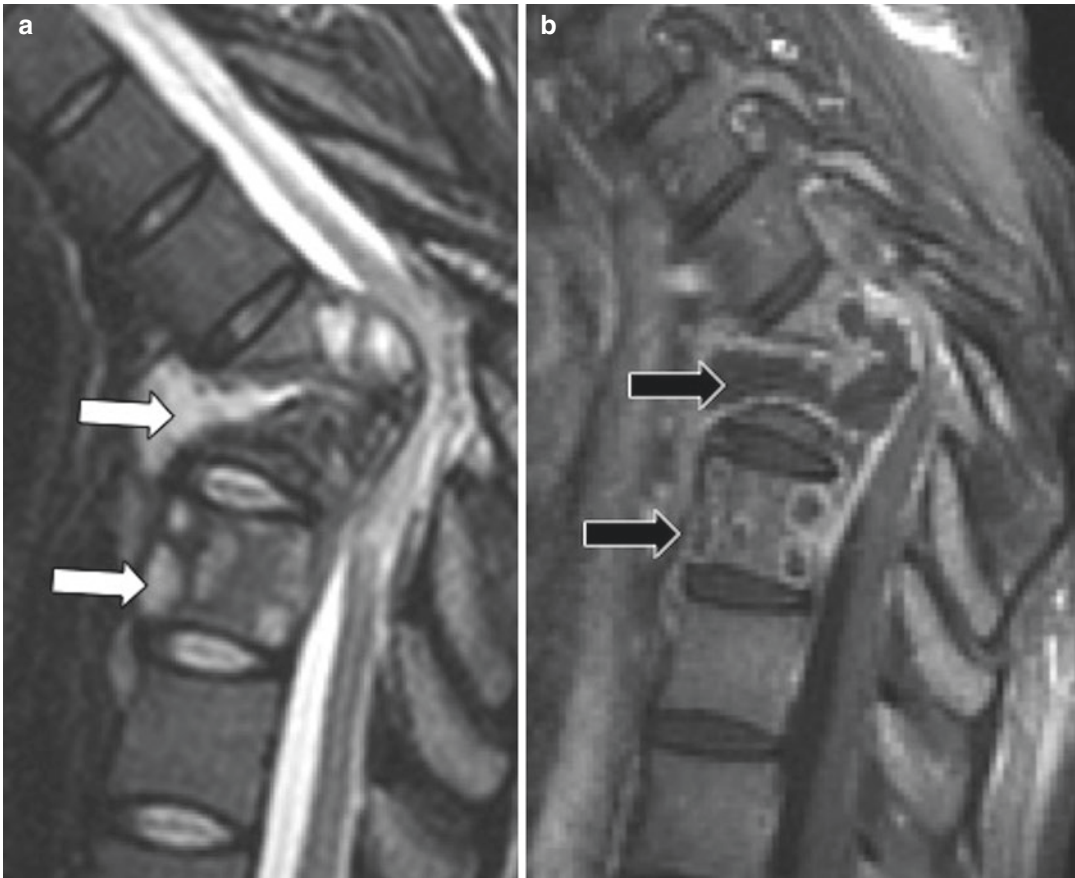


Fig. 5.10 A 37-year-old female with tuberculous spondylodiscitis. Sagittal STIR fat-saturated image (**a**) and sagittal T1 fat-saturated post-contrast image (**b**) demon-

strate hyperintense T2 foci within the mid-thoracic vertebra (white arrow) with thin peripheral enhancement in keeping with intraosseous abscesses (black arrow)

Fungal Spondylodiscitis

Pathophysiology

Similar to tuberculous spondylodiscitis, fungal spondylodiscitis tends to present with an indolent course in contrast to pyogenic spondylodiscitis. Patients with immune compromise, diabetics, and postoperative patients are at a higher risk of developing the disease and often present with vague symptoms of back pain without fever or profound leukocytosis. The most common fungi isolated in spondylodiscitis fall in the *Candida*, *Aspergillus*,

and *Mucor* genus. Yet there are regional predilections that introduce other more exotic species. Histoplasmosis infection, for example, is seen in higher number in the Midwest states (Indiana, Arkansas). Blastomycosis is more common in Mississippi and Wisconsin with coccidioidomycosis seen in the Western United States (Arizona, California) [36]. Although the immune-compromised patient is most commonly affected, reports of aggressive fungal infection have been described in otherwise healthy immune-competent patients, and the consideration of fungal etiologies can be considered in all patient populations.

Imaging in Fungal Spondylodiscitis

Radiographs

Fungal infection in the spine is the great mimicker of spinal infections with imaging similar to pyogenic infection, tuberculous infection, or even, in some instances, malignancy. Radiographic appearance in fungal disease is therefore quite broad and non-specific. Again, because of the absence of proteolytic enzymes, a sub-ligamentous, disc sparing pattern mimicking that of tuberculous spondylodiscitis is the most common presentation. Radiographs may demonstrate the classic vertebral collapse and Gibbus deformity seen also in TS.

Magnetic Resonance Imaging

MRI is the gold standard imaging for the detection of the often subtle imaging findings in fungal disease. T1 and T2 signal abnormalities are similar to that of other infections but may be even more faint due to the relatively mild inflammatory response initiated by the fungal elements [37]. Various fungal organisms result in different presentations on imaging. For example, *Candida* species, the most common fungal organism isolated in spondylodiscitis, typically involves the lumbar spine and mimics that of pyogenic infection primarily with disc involvement and endplate erosions [37, 38] (Fig. 5.11). Disc destruction is seen in about 50% of *Candida* cases but is thought to be a common feature in many fungal infections. *Aspergillus* and *Blastomyces* infections have a propensity to involve multiple and sometimes non-contiguous vertebral levels, resulting in enhancement of the ligamentous structures themselves in addition to sub-ligamentous spread [39, 40] (Fig. 5.12).

Suspicion for fungal infection should increase if MRI shows spondylitis in two adjacent vertebral bodies with small paraspinous abscess. These abscesses in fungal infection can be differentiated from the typical and atypical bacterial abscesses in the degree of internal complexity and intermediate T2-weighted signal in contrast to the hyperintensity expected in pyogenic or tuberculosis infection. Clear disc destruction with a notable absence of T2 signal within the intervertebral disc involvement may also suggest

fungal rather than pyogenic spondylitis [41]. This absence of T2 signal in the disc is thought to be related to paramagnetic and ferromagnetic elements within the fungi themselves, which alter the relaxation times and thus signal intensity of T2-weighted imaging [42].

A rare but interesting manifestation of fungal disease is that of multifocal marrow lesions that may easily be mistaken for metastatic disease [43] (Fig. 5.13).

Brucella Spondylodiscitis

Pathophysiology

Spine infection is caused by a wide array of organisms including the *Brucella* species. Brucellosis is a zoonotic infection caused by Gram-negative bacilli from the *Brucella* genus. *Brucella* is transmitted to human through contact with unpasteurized, contaminated milk products [44, 45].

In endemic areas, spondylodiscitis is caused by the *Brucella* organism in an impressive 35–48% of cases [46, 47]. Even in non-endemic areas like the United States, this organism should be considered in the differential of spine infection. *Brucella* spondylodiscitis is worthy of independent discussion because of the unique features this has on treatment. The most appropriate and effective treatment of *Brucella* spondylodiscitis is still unknown, and management of these patients can be difficult [46]. Clinical improvement can lag behind treatment initiation by up to 12 weeks, and a high rate of treated patients ultimately fail therapy (25%) [46–49].

Brucella most commonly affects male patients over 50 years of age and classically patients residing in rural areas with occupational risk factors. Despite this, as the disease process and our understanding of the illness evolves, the classic patient population becomes more broad, now often seen in women from urban areas without risk factors for the disease [46, 48].

The most affected spinal segment is lumbar (50–80%) followed by the thoracic and cervical spine. Involvement of one spinal level (two

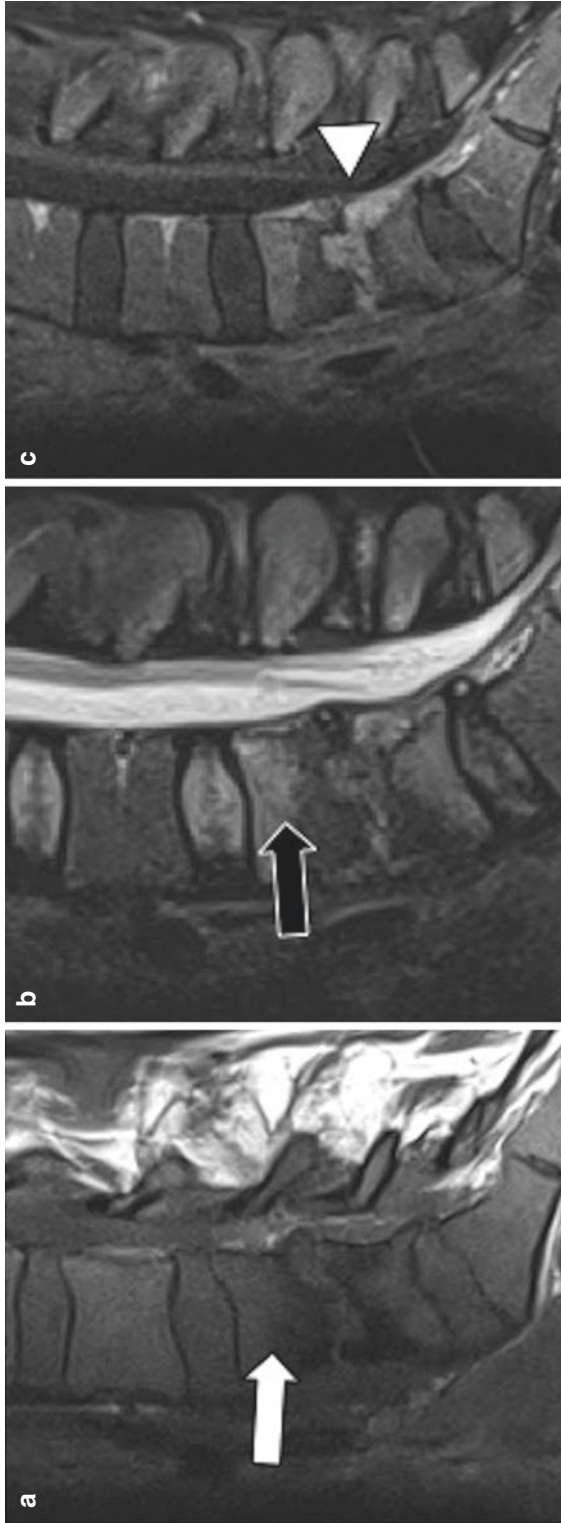


Fig. 5.11 A 67-year-old male with *Candida* spondylodiscitis. Sagittal T1 (a), STIR fat-saturated (b), and T1 fat-saturated post-contrast (c) images demonstrate findings similar to pyogenic spondylodiscitis with disc height loss, confluent hypointense T1 signal (white arrow), and hyperintense T2 signal (black arrow) with disc and epidural enhancement (white arrowhead)

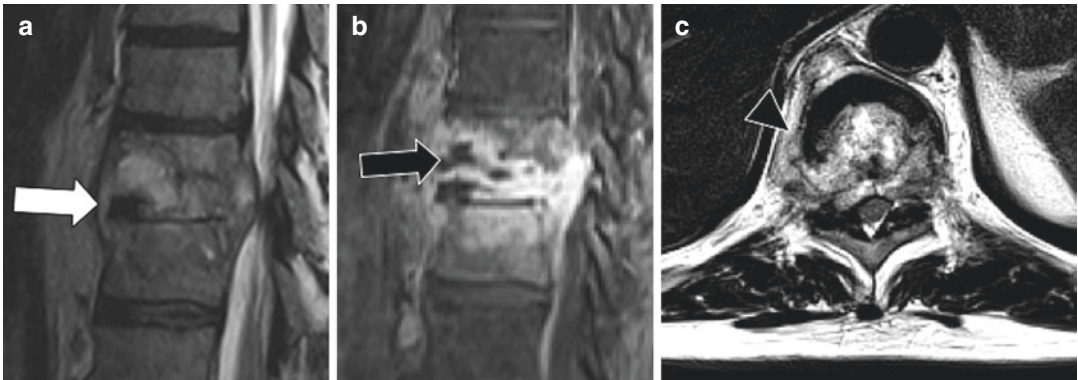


Fig. 5.12 A 49-year-old male with *Aspergillus* spondylodiscitis. Sagittal T2 (a), T1 fat-saturated post-contrast (b), and axial T2 (c) images of the spine demonstrate T9 and T10 vertebral edema with enhancement and subligamentous hyperintense T2 signal (white arrow) as well

as peripheral rim-enhancing intravertebral abscess (black arrow). Imaging mimics tuberculous spondylodiscitis but with features more in keeping with fungal disease including disc height loss and a complex T2 paraspinous abscess (black arrowhead)

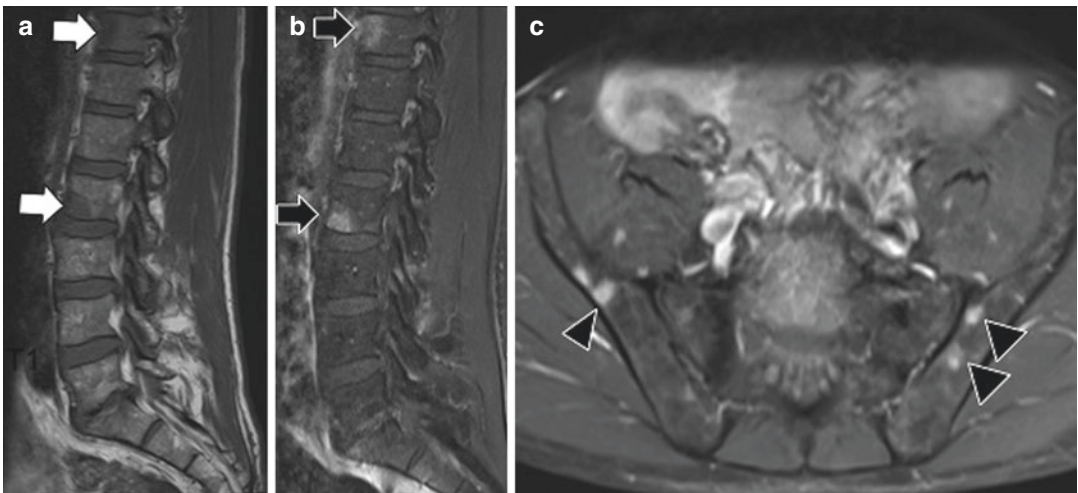


Fig. 5.13 A 63-year-old with disseminated coccidiomycosis. Sagittal T1 (a), sagittal T1 fat-saturated post-contrast (b), and axial T1 fat-saturated post-contrast (c) images demonstrate multifocal hypointense T1, enhanc-

ing lesions throughout the spine and pelvis, mimicking metastatic disease. Lesions were biopsied and shown to be disseminated coccidiomycosis

consecutive vertebrae) is the most common presentation. However, multifocal consecutive and non-consecutive involvement has been described. Both epidural and paraspinous abscesses have been seen in the setting of *Brucella* spine infection [46, 48, 49].

Imaging of *Brucella* Spondylodiscitis

Differentiating *Brucella* spondylodiscitis from other infectious spondylodiscitis can be exceed-

ingly difficult due to the overlap in imaging findings. The most common MRI features of *Brucella* spondylodiscitis include osseous hypointense T1 signal, hyperintense T2 signal, diffuse enhancement, disc height loss with endplate destruction, and presence or absence of epidural or paraspinous abscesses. Characteristic MRI features of *Brucella* spondylodiscitis have been described and include the preservation of vertebral architecture despite extensive marrow involvement, profound increased signal in the intervertebral disc, and facet joint involvement

[48, 50]. Unfortunately none of these features are pathognomonic for the disease, and clinical history and risk factors may arguably be the most important features for the assumption of the diagnosis.

Infectious Spondylodiscitis Versus Degeneration

Degenerative disc disease and neuropathic (Charcot) spine often present with similar MRI signal changes to infectious spondylodiscitis creating intricacy in differentiating these entities. Further compounding the muddled imaging picture is the propensity of bacterial pathogens to preferentially seed degenerative discs over normal discs. Ingrowth of vascularized granulation tissue occurs with intervertebral disc desiccation owing to increased blood flow resulting in higher risk of bacterial seeding. While a few of the defining imaging features of infectious and degenerative discitis have been discussed, there are other defining features of these conditions that should be considered when attempting to narrow the differential diagnosis in patients with back pain.

Neuropathic (Charcot) spine is a condition whereby the vertebral facets and intervertebral discs become denervated owing to a rapid and often profound degeneration of the spine with subsequent inflammatory imaging features and pain. Because of the degree of bony destruction, endplate irregularities, and inflammation, differentiating this condition from the aggressive infectious spondylodiscitis is difficult. On CT and radiography, features suggestive of neuropathic spine include involvement of the vertebral facet joints, osseous debris around the vertebra, spondylolisthesis, and intradiscal vacuum phenomenon [51] (Fig. 5.14).

The finding of intradiscal vacuum phenomenon is a common finding, which deserves additional consideration. In this condition, gas bubbles, usually nitrogen, are removed from solution through a negative pressure mechanism and accumulate within the intervertebral discs [52]. The notion that vacuum phenomenon

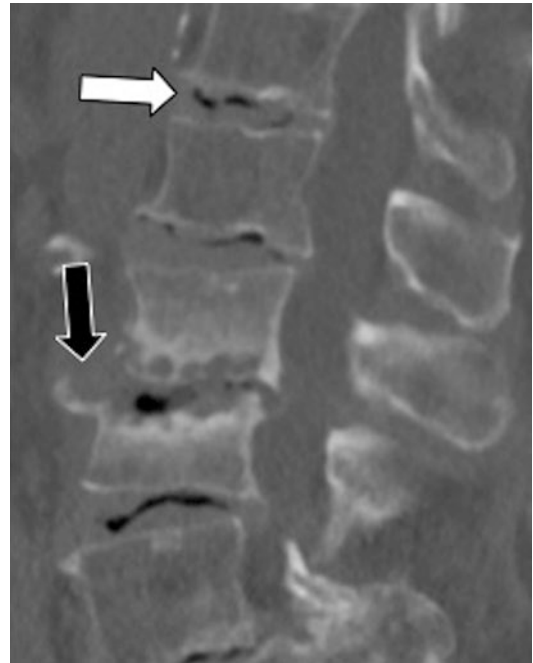


Fig. 5.14 Sagittal CT image of the lumbar spine in a patient with neuropathic/Charcot spine demonstrates multilevel intradiscal vacuum phenomenon (white arrow) and bony debris (black arrow)

excludes the possibility of infectious discitis is widely debated in the literature. Many reports suggest that intradiscal vacuum phenomenon is an indication of benign conditions (i.e., neuropathic spine, osteonecrosis, and vertebral compression fracture), occurring as a result of negative pressure across the disc space [51, 53, 54]. In spine infection, the influx of inflammatory cells into the discs, vertebra, and adjacent soft tissues creates a positive pressure environment that is not conducive to the formation of the vacuum effect. Although case reports of intradiscal gas in the setting of infection exist, the incidence of this finding is exceedingly rare [55, 56]. In a report examining 307 patients with known disc infection, intradiscal gas was identified in only 1 patient (0.003%) [53]. Despite the low incidence of infectious related intradiscal gas, some degree of caution should be applied when interpreting this finding especially when the distribution and the morphology of the gas are heterogeneous, nonlinear, or otherwise atypical in appearance.

Several advanced MR imaging techniques proposed in the literature have shown promise in differentiating degenerative and infectious discitis. Diffusion-weighted imaging (DWI), for example, is an established technique in brain imaging that has recently been adapted to the spine as a means to differentiate Modic endplate edema from infection. Authors suggest that degenerative Modic edema restricts in a linear sub-endplate morphology creating a “claw sign” on DWI. Infection, by contrast, restricts more diffusely through the vertebra [57].

Berry et al. in 2009 described an advanced MR imaging technique that uses iron oxide injection to aid in the determination of endplate edema. In this technique, supra-paramagnetic iron oxide particles are injected intravenously and phagocytized by macrophages, ultimately resulting in an iron oxide accumulation along the endplates of infected vertebra. The supra-paramagnetic properties of iron oxide result in a post-injection T2 signal dropout along the infected endplates, a finding absent in the setting of degenerative Modic edema [58].

Sacroiliac Joint Septic Arthritis

Pathophysiology

Disorders of the sacroiliac joint include degenerative, traumatic, inflammatory, and infectious etiologies. Inflammatory sacroiliitis is seen with some frequency in both seronegative and seropositive arthropathies and is almost always bilateral and symmetric, a key imaging feature of this disease process. Unilateral inflammatory sacroiliitis, however, has been described in both, posing a challenge when differentiating inflammatory from septic arthritis [59].

Infectious sacroiliitis is a relatively uncommon condition making up only 1–4% of all cases of sacroiliac arthritis [60]. Most cases are caused by hematogenous spread of bacteria, but direct inoculation from adjacent infection, deep sacral ulceration, or instrumentation has also been described [61]. The typical presentation of septic sacroiliitis includes low back pain, sciatica,

fevers, and elevated inflammatory markers. These are relatively non-specific findings often overlapping the clinical presentations of other diseases such as acute spondyloarthropathy, lumbar degenerative disease, diverticulitis, or appendicitis. Evaluation with MRI or CT has been shown to be useful in the diagnosis of septic arthritis but requires a sophisticated understanding of the imaging subtleties as to not confuse the imaging with that of unilateral inflammatory sacroiliitis [61, 62].

Imaging

Radiographic findings of septic sacroiliitis are often subtle and include periarticular osteopenia and erosions. Differentiating infection from inflammatory sacroiliitis on radiography is largely dependent on the unilateral nature of the sacroiliac joint involvement. When considering the possibility of unilateral inflammatory disease, for example, psoriasis or unilateral ankylosing spondylitis, radiographs can be non-specific.

MRI is arguably the most sensitive imaging modality for the differentiation of inflammatory and infectious sacroiliitis. Kang et al. found that the most accurate independent variable identified in these patients is the presence of periarticular edema and iliopsoas muscle swelling [63]. Fluid signal tracking along the muscle belly and intermuscular fat planes of the pelvic side wall on fluid-sensitive MRI sequences corresponded to a high accuracy and specificity for the diagnosis of septic arthritis in other studies as well [62–64] (Fig. 5.15)

The pattern of bone marrow edema may also be helpful in determining the origin of the inflammation. A well-established feature of seronegative spondyloarthropathy is the iliac predominant bone marrow edema pattern that occurs early in the disease process. The iliac predominance is thought to be related to the differences in the makeup of sacral and iliac cartilage with the iliac fibrocartilage layer serving as an enthesis that is prone to inflammation in conditions like ankylosing spondylitis [63, 65]. In the setting of infection, both the sacral hyaline cartilage and

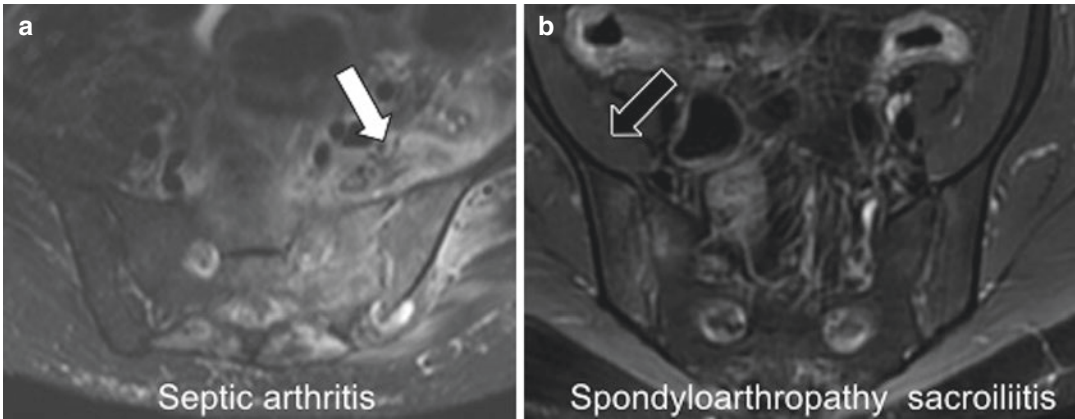


Fig. 5.15 Axial T2 fat-saturated images in a patient with septic arthritis (**a**) demonstrate profound hyperintense T2 signal within and around the iliopsoas muscle and pelvic side wall (white arrow). T2 fat-saturated images in a

patient with ankylosing spondylitis and inflammatory sacroiliitis (**b**) demonstrate bone marrow edema with a notable absence of periarticular pelvic side wall edema (black arrow)

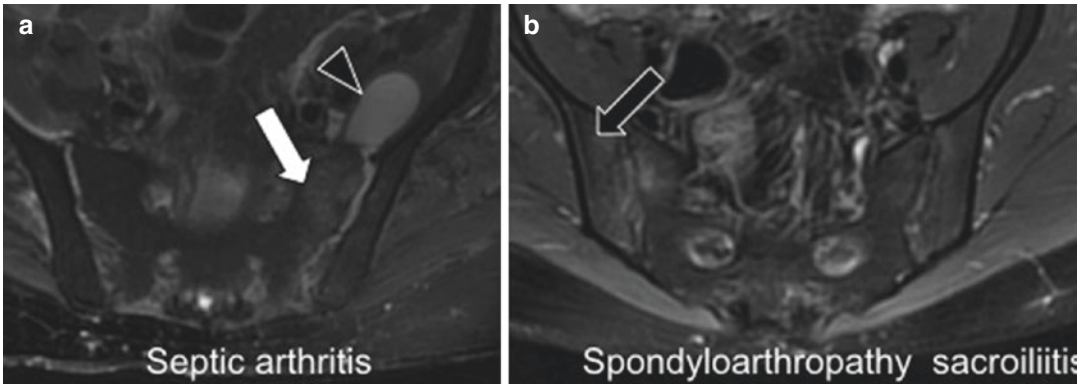


Fig. 5.16 Axial T2 fat-saturated images in a patient with septic arthritis (**a**) demonstrate sacral predominant bone marrow manifesting as hyperintense T2 signal (white arrow). The presence of a large pericapsular hyperintense T2 fluid collection (black arrowhead) favors the diagnosis

of septic arthritis. T2 fat-saturated images in a patient with ankylosing spondylitis and inflammatory sacroiliitis (**b**) demonstrate the classic iliac predominant bone marrow edema (black arrow)

the iliac fibrocartilage are equally susceptible to inflammation. This manifests in a unique sacral predominant or equal sacral and iliac bone marrow edema pattern in septic arthritis [65] (Fig. 5.16).

Extracapsular fluid collections are seen exclusively in septic arthritis and when present should be considered highly suspicious for infection. Other features favoring septic arthritis include large subchondral erosions and thick capsulitis with absence of joint enhancement [62, 63]. The imaging findings in septic versus inflammatory sacroiliitis are illustrated in Table 5.2.

Table 5.2 MR imaging features of septic versus inflammatory sacroiliitis [63]

MR imaging feature	Septic sacroiliitis	Inflammatory sacroiliitis
Bone marrow edema	Sacral predominant, equal sacral and iliac edema	Iliac predominant edema
Periarticular soft tissue edema	Severe, often extending into the iliopsoas muscle and pelvic side wall	Mild or non-existent
Capsulitis	Severe	Mild
Periarticular fluid collection	Present	Absent
Subchondral erosions	Large (>1 cm), irregular	Small, uniform

Epidural Abscess

Pathophysiology

Epidural abscess refers to an infectious fluid collection contained between the dura of the thecal sac and the periosteum of the adjacent bone. The incidence of epidural abscess is about 2–3 per 100,000 hospital admissions and is seen most frequently in the fifth to seventh decades of life [66]. Risk factors for the formation of epidural abscesses include diabetes, intravenous drug abuse, immune compromise, and recent intervention. While hematogenous seeding of the epidural space does occur, epidural abscess most commonly forms as a direct extension of infection from adjacent osteomyelitis/discitis [67].

Failure of medical treatment is unfortunately common, especially in the setting of diabetes and bacteremia. Prompt identification of epidural abscess and initiation of therapy, either medical or surgical, is imperative to treatment success [68]. Epidural abscesses, when hematogenously spread, usually occur at the dorsal epidural space and have a propensity to affect multiple levels of the spine resulting in “skip lesions” along the neural axis. For this reason, whole spine imaging is recommended in patients

with known or suspected hematogenously spread epidural infection [68, 69].

Imaging

MRI is the modality of choice for the evaluation of epidural abscess, offering superior spatial resolution and sensitivity [70]. Although non-contrast MRI has reasonable sensitivity in the detection of epidural disease, the addition of post-contrast images increases sensitivity and specificity over non-contrast images alone and should be preferentially performed in all cases of suspected epidural abscess [71].

There are two main imaging appearances of epidural abscess, differing in signal characteristics and enhancement based on the age of the lesion. The first imaging pattern is seen in the early phlegmonous stages of infection. In this phase, the epidural abscess is made up of predominantly thick enhancing granulation tissue that appears as a confluent but often heterogeneous hyperintense T2 signal epidural mass with diffuse internal enhancement (Fig. 5.17). As the epidural abscess matures, the central areas of granulation become necrotic and fluid-like, appearing as homogeneous hyperintense T2 signal with thick peripheral enhancement [67, 72] (Fig. 5.18).

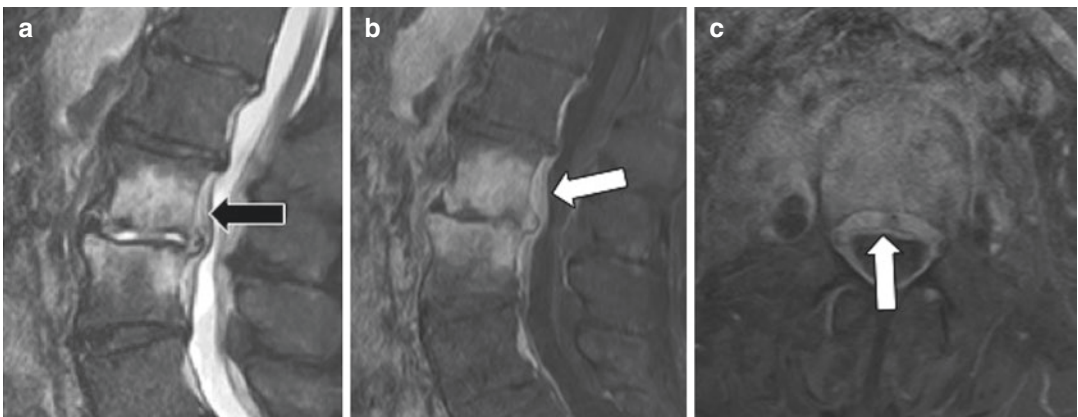


Fig. 5.17 A 67-year-old male with L2–L3 spondylodiscitis and early epidural abscess. Sagittal STIR fat-saturated (a), sagittal T1 fat-saturated post-contrast (b), and axial T1 fat-saturated post-contrast images (c) dem-

onstrate focal thickening of the ventral epidural space posterior to the L2–L3 disc. There is heterogeneous T2 signal (black arrow) and internal enhancement (white arrows)

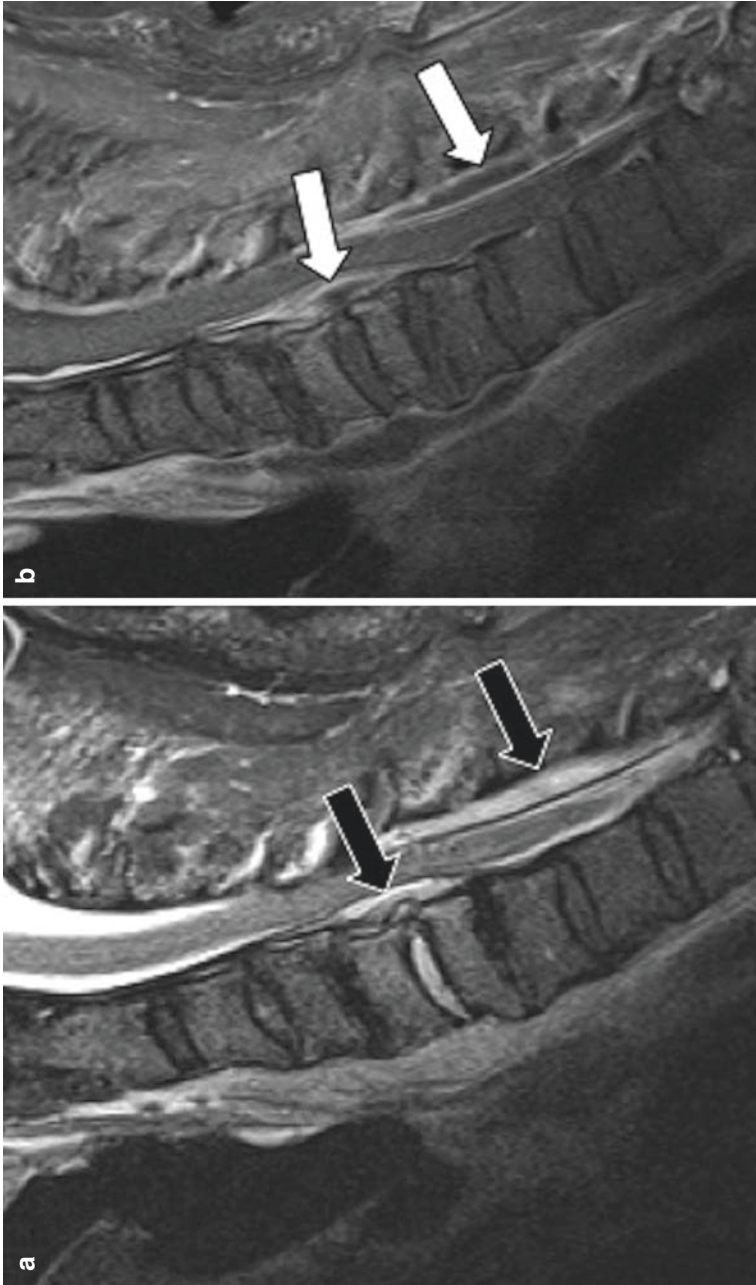


Fig. 5.18 A 50-year-old male IV drug abuser with neck pain. Sagittal STIR fat-saturated (a) and T1 fat-saturated post-contrast images (b) demonstrate C5–C6 spondylodiscitis with an adjacent ventral epidural abscess as well as a secondary dorsal abscess “skip lesion.” The abscesses are mature demonstrating hyperintense T2 signal (black arrows) with peripheral enhancement (white arrows) indicative of central necrotic avascular material

Conclusion

Spine infection is unfortunately a common occurrence, especially in susceptible patient populations. While the imaging findings in spine infection are not always subtle, differentiating findings of infection from other disease processes can be extremely difficult. A sophisticated understanding of the unique imaging features in both infectious and non-infectious disease processes is critical to the accurate diagnosis and prompt treatment of this high-risk patient population.

References

- Berhouma M, Krolak-Salmon P, editors. *Brain and spine surgery in the elderly*. Cham: Springer; 2017. p. 305–27.
- Cramer J, Haase N, Behre I, Ostermann PAW. Spondylitis und Spondylodiszitis. *Trauma und Berufskrankheit*. 2003;5:336–41.
- Stoffel M, Hecker J, Ringel F, Meyer B, Stürer C. A staged treatment algorithm for spinal infections. *J Neurol Surg Part A*. 2013;74:087–95.
- Nolla JM, Ariza J, Gómez-Vaquero C, Fiter J, Bermejo J, Valverde J, Escofet DR, Gudiol F. Spontaneous pyogenic vertebral osteomyelitis in nondrug users. *Semin Arthritis Rheum*. 2002;31:271–8.
- Mchenry MC, Easley KA, Locker GA. Vertebral osteomyelitis: long-term outcome for 253 patients from 7 cleveland-area hospitals. *Clin Infect Dis*. 2002;34:1342–50.
- Karadimas EJ, Bunger C, Lindblad BE, Hansen ES, Høy K, Helmig P, Kannerup AS, Niedermann B. Spondylodiscitis. A retrospective study of 163 patients. *Acta Orthop*. 2008;79:650–9.
- Waldvogel FA, Medoff G, Swartz MN. Osteomyelitis: a review of clinical features, therapeutic considerations and unusual aspects. *N Engl J Med*. 1970;282:198–206.
- Gouliouris T, Aliyu SH, Brown NM. Spondylodiscitis: update on diagnosis and management – authors responses. *J Antimicrob Chemother*. 2011;66:1200–2.
- Ratcliffe JF. Anatomic basis for the pathogenesis and radiologic features of vertebral osteomyelitis and its differentiation from childhood discitis. *Acta Radiologica Diagnosis*. 1985;26:137–43.
- Maiuri F, Laconetta G, Gallicchio B, Manto A, Briganti F. Spondylodiscitis-. *Spine*. 1997;22:1741–6.
- Cheung WY, Luk KDK. Pyogenic spondylitis. *Int Orthop*. 2011;36:397–404.
- Pineda C, Vargas A, Rodríguez AV. Imaging of osteomyelitis: current concepts. *Infect Dis Clin N Am*. 2006;20:789–825.
- Hadjipavlou AG, Cesani-Vazquez F, Villaneuva-Meyer J. The effectiveness of gallium citrate Ga 67 radionuclide imaging in vertebral osteomyelitis revisited. *Am J Orthop*. 1998;27:179–83.
- Smids C, Kouijzer IJE, Vos FJ, Sprong T, Hosman AJF, Rooy JWJD, Aarntzen EHJG, Geus-Oei L-FD, Oyen WJG, Bleeker-Rovers CP. A comparison of the diagnostic value of MRI and 18F-FDG-PET/CT in suspected spondylodiscitis. *Infection*. 2016;45:41–9.
- Leone A, Dell'Atti C, Magarelli N, Colelli P, Balanika A, Casale R, Bonomo L. Imaging of spondylodiscitis. *Eur Rev Med Pharmacol Sci*. 2012;16(Suppl 2):8–19.
- Modic MT, Feiglin DH, Piraino DW, Boumpfrey F, Weinstein MA, Duchesneau PM, Rehm S. Vertebral osteomyelitis: assessment using MR. *Radiology*. 1985;157:157–66.
- Modic MT, Steinberg PM, Ross JS, Masaryk TJ, Carter JR. Degenerative disk disease: assessment of changes in vertebral body marrow with MR imaging. *Radiology*. 1988;166:193–9.
- Luoma K, Vehmas T, Grönblad M, Kerttula L, Kääpä E. Relationship of Modic type 1 change with disc degeneration: a prospective MRI study. *Skelet Radiol*. 2008;38:237–44.
- Ledermann HP, Schweitzer ME, Morrison WB, Carrino JA. MR imaging findings in spinal infections: rules or myths? *Radiology*. 2003;228:506–14.
- Varma R, Lander P, Assaf A. Imaging of pyogenic infectious spondylodiskitis. *Radiol Clin N Am*. 2001;39:203–13.
- Yeom JA, Lee IS, Suh HB, Song YS, Song JW. Magnetic resonance imaging findings of early spondylodiscitis: interpretive challenges and atypical findings. *Korean J Radiol*. 2016;17:565.
- Desanto J, Ross JS. Spine infection/inflammation. *Radiol Clin N Am*. 2011;49:105–27.
- Dunbar J, Sandoe J, Rao A, Crimmins D, Baig W, Rankine J. The MRI appearances of early vertebral osteomyelitis and discitis. *Clin Radiol*. 2010;65:974–81.
- Carragee EJ. The clinical use of magnetic resonance imaging in pyogenic vertebral osteomyelitis. *Spine*. 1997;22:780–5.
- Zarrouk V, Feydy A, Salles F, Dufour V, Guigui P, Redondo A, Fantin B. Imaging does not predict the clinical outcome of bacterial vertebral osteomyelitis. *Rheumatology*. 2006;46:292–5.
- Gillams AR, Chaddha B, Carter AP. MR appearances of the temporal evolution and resolution of infectious spondylitis. *Am J Roentgenol*. 1996;166:903–7.
- Kowalski TJ, Barbari EF, Huddleston PM, Steckelberg JM, Osmon DR. Do follow-up imaging examinations provide useful prognostic information in patients with spine infection? *Clin Infect Dis*. 2006;43:172–9.
- Watson JM. Tuberculosis in Britain today. *BMJ*. 1993;306:221–2.
- Tsiodras S, Falagas ME. Clinical assessment and medical treatment of spine infections. *Clin Orthop Relat Res*. 2006;443:38–50.

30. Koo K-H, Lee H-J, Chang B-S, Yeom J-S, Park K-W, Lee C-K. Differential diagnosis between tuberculous spondylitis and pyogenic spondylitis. *J Korean Soc Spine Surg.* 2009;16:112.
31. Lee KY. Comparison of pyogenic spondylitis and tuberculous spondylitis. *Asian Spine J.* 2014;8:216.
32. Jung N-Y, Jee W-H, Ha K-Y, Park C-K, Byun J-Y. Discrimination of tuberculous spondylitis from pyogenic spondylitis on MRI. *Am J Roentgenol.* 2004;182:1405–10.
33. Chang M-C, Wu HTH, Lee C-H, Liu C-L, Chen T-H. Tuberculous spondylitis and pyogenic spondylitis. *Spine.* 2006;31:782–8.
34. Alothman A, Memish ZA, Awada A, Mahmood SA, Sadoon SA, Rahman MM, Khan MY. Tuberculous spondylitis. *Spine.* 2001;26:E565. <https://doi.org/10.1097/00007632-200112150-00020>.
35. Shanley DJ. Tuberculosis of the spine: imaging features. *Am J Roentgenol.* 1995;164:659–64.
36. Baddley J. Geographic distribution of endemic fungal infections among older persons, United States. *Emerg Infect Dis.* 2011;17:1664–9.
37. Frazier DD, Campbell DR, Garvey TA, Wiesel S, Bohlman HH, Eismont FJ. Fungal infections of the spine. *J Bone Joint Surg Am Vol.* 2001;83:560–5.
38. Kim CW, Perry A, Currier B, Yaszemski M, Garfin SR. Fungal infections of the spine. *Clin Orthop Relat Res.* 2006;444:92–9.
39. Dotis J, Roilides E. Osteomyelitis due to *Aspergillus* species in chronic granulomatous disease: an update of the literature. *Mycoses.* 2011;54:e686. <https://doi.org/10.1111/j.1439-0507.2010.02001.x>.
40. Horn D, Sae-Tia S, Neofytos D. *Aspergillus* osteomyelitis: review of 12 cases identified by the prospective antifungal therapy Alliance registry. *Diagn Microbiol Infect Dis.* 2009;63:384–7.
41. Lee S-W, Lee SH, Chung HW, Kim MJ, Seo MJ, Shin MJ. Candida spondylitis: comparison of MRI findings with bacterial and tuberculous causes. *Am J Roentgenol.* 2013;201:872–7.
42. Williams RL, Fukui MB, Meltzer CC, Swarnkar A, Johnson DW, Welch W. Fungal spinal osteomyelitis in the immunocompromised patient: MR findings in three cases. *AJNR Am J Neuroradiol.* 1999;20:381–5.
43. McConnell MF, Shi A, Lasco TM, Yoon L. Disseminated coccidioidomycosis with multifocal musculoskeletal disease involvement. *Radiol Case Rep.* 2017;12:141–5.
44. Tekkök IH, Berker M, Özcan OE, Özgen T, Akalin E. Brucellosis of the spine. *Neurosurgery.* 1993;33:838–44.
45. Gotuzzo E, Seas C, Guerra JG, Carrillo C, Bocanegra TS, Calvo A, Castaneda O, Alarcon GS. Brucellar arthritis: a study of 39 Peruvian families. *Ann Rheum Dis.* 1987;46:506–9.
46. Colmenero JD, Jimenez-Mejias ME, Sanchez-Lora FJ, Reguera JM, Palomino-Nicas J, Martos F, Heras JGD, Pachon J. Pyogenic, tuberculous, and brucellar vertebral osteomyelitis: a descriptive and comparative study of 219 cases. *Ann Rheum Dis.* 1997;56:709–15.
47. Sakkas LI, Davas EM, Kapsalaki E, Boulbou M, Makaritsis K, Alexiou I, Tsirikas T, Stathakis N. Hematogenous spinal infection in Central Greece. *Spine.* 2009;34:E513. <https://doi.org/10.1097/brs.0b013e3181a9897e>.
48. Kaptan F, Gulduren HM, Sarsilmaz A, Sucu HK, Ural S, Vardar I, Coskun NA. Brucellar spondylodiscitis: comparison of patients with and without abscesses. *Rheumatol Int.* 2012;33:985–92.
49. Solera J, Lozano E, Martinez-Alfaro E, Espinosa A, Castillejos ML, Abad L. Brucellar spondylitis: review of 35 cases and literature survey. *Clin Infect Dis.* 1999;29:1440–9.
50. Özaksoy D, Yücesoy K, Yücesoy M, Kovanlıkaya I, Yüce A, Naderi S. Brucellar spondylitis: MRI findings. *Eur Spine J.* 2001;10:529–33.
51. Wagner SC, Schweitzer ME, Morrison WB, Przybylski GJ, Parker L. Can imaging findings help differentiate spinal neuropathic arthropathy from disk space infection? Initial experience. *Radiology.* 2000;214:693–9.
52. Resnick D, Niwayama G, Guerra J, Vint V, Usselman J. Spinal vacuum phenomena: anatomical study and review. *Radiology.* 1981;139:341–8.
53. Feng S-W, Chang M-C, Wu H-T, Yu J-K, Wang S-T, Liu C-L. Are intravertebral vacuum phenomena benign lesions? *Eur Spine J.* 2011;20:1341–8.
54. Libicher M, Appelt A, Berger I, Baier M, Meeder P-J, Grafe I, Dafonseca K, Nöldge G, Kasperk C. The intravertebral vacuum phenomenon as specific sign of osteonecrosis in vertebral compression fractures: results from a radiological and histological study. *Eur Radiol.* 2007;17:2248–52.
55. Pate D, Katz A. Clostridia discitis: a case report. *Arthritis Rheum.* 1979;22:1039–40.
56. Bielecki D, Sartoris D, Resnick D, Lom KV, Fierer J, Haghighi P. Intraosseous and intradiscal gas in association with spinal infection: report of three cases. *Am J Roentgenol.* 1986;147:83–6.
57. Patel KB, Poplawski MM, Pawha PS, Naidich TP, Tanenbaum LN. Diffusion-weighted MRI “claw sign” improves differentiation of infectious from degenerative Modic type 1 signal changes of the spine. *Am J Neuroradiol.* 2014;35:1647–52.
58. Bierry G, Jehl F, Holl N, Sibilia J, Froelich S, Froehlig P, Dietemann J-L, Kremer S. Cellular magnetic resonance imaging for the differentiation of infectious and degenerative vertebral disorders: preliminary results. *J Magn Reson Imaging.* 2009;30:901–6.
59. Canella C, Schau B, Ribeiro E, Sbaffi B, Marchiori E. MRI in seronegative spondyloarthritis: imaging features and differential diagnosis in the spine and sacroiliac joints. *Am J Roentgenol.* 2013;200:149–57.
60. Forrester D, Kilcoyne R. Osteomyelitis and septic arthritis. *Musculoskelet Dis.* 2005:138–42.
61. Resnick D, Kransdorf MJ. Osteomyelitis, septic arthritis, and soft tissue infection: axial skeleton. *Bone Joint Imaging.* 2005:743–52.
62. Klein MA, Winalski CS, Wax MR, Pivnicka-Worms DR. MR imaging of septic sacroiliitis. *J Comput Assist Tomogr.* 1991;15:126–32.

63. Kang Y, Hong SH, Kim JY, Yoo HJ, Choi J-Y, Yi M, Kang HS. Unilateral sacroiliitis: differential diagnosis between infectious sacroiliitis and spondyloarthritis based on MRI findings. *Am J Roentgenol*. 2015;205:1048–55.
64. Sandrasegaran K, Saifuddin A, Coral A, Butt WP. Magnetic resonance imaging of septic sacroiliitis. *Skelet Radiol*. 1994;23:289–92.
65. Prabhu S, Irodi A, Prakash D. Seronegative spondyloarthropathy-related sacroiliitis: CT, MRI features and differentials. *Indian J Radiol Imaging*. 2014;24:271.
66. Reihnsaus E, Waldbaur H, Seeling W. Spinal epidural abscess: a meta-analysis of 915 patients. *Neurosurg Rev*. 2000;23:175–204.
67. Darouiche RO. Spinal epidural abscess. *N Engl J Med*. 2006;355:2012–20.
68. Patel AR, Alton TB, Bransford RJ, Lee MJ, Bellabarba CB, Chapman JR. Spinal epidural abscesses: risk factors, medical versus surgical management, a retrospective review of 128 cases. *Spine J*. 2014;14:326–30.
69. Ju KL, Kim SD, Melikian R, Bono CM, Harris MB. Predicting patients with concurrent noncontiguous spinal epidural abscess lesions. *Spine J*. 2015;15:95–101.
70. Laur O, Mandell JC, Titelbaum DS, Cho C, Smith SE, Khurana B. Acute nontraumatic back pain: infections and mimics. *Radiographics*. 2019;39(1):287–8.
71. Dillon WP, Norman D, Newton TH, Bolla K, Mark A. Intradural spinal cord lesions: Gd-DTPA-enhanced MR imaging. *Radiology*. 1989;170:229–37.
72. Numaguchi Y, Rigamonti D, Rothman MI, Sato S, Mihara F, Sadato N. Spinal epidural abscess: evaluation with gadolinium-enhanced MR imaging. *Radiographics*. 1993;13:545–59.